Radiotherapy and Oncology 123 (2017) 176–181

Contents lists available at ScienceDirect

Radiotherapy and Oncology

journal homepage: www.thegreenjournal.com

Radiation induced rib fractures

Dose–effect analysis of radiation induced rib fractures after thoracic SBRT

Barbara Stam, Erik van der Bijl, Heike Peulen, Maddalena M.G. Rossi, José S.A. Belderbos, Jan-Jakob Sonke *

Department of Radiation Oncology, Netherlands Cancer Institute, Amsterdam, The Netherlands

ARTICLE INFO

Article history:
Received 29 August 2016
Received in revised form 30 December 2016
Accepted 3 January 2017
Available online 19 January 2017

Keywords:
Rib fracture
SBRT
NTCP
Lung cancer
Dose–effect

ABSTRACT

Background and purpose: To determine a dose–effect relation for radiation induced rib fractures after stereotactic body radiation therapy (SBRT) in early stage non-small cell lung cancer (NSCLC). Automatic rib delineation has enabled the analysis of a large patient group.

Material and methods: Four-hundred and sixty-six patients with stage I/II NSCLC received SBRT with a median of 54 Gy in 3 fractions. The optimal EQD2-corrected dose parameter to predict (a)symptomatic fractures was found using Cox regression. Three normal tissue complication probability (NTCP) models based on this optimal parameter were constructed: (1) at a median follow up (FU) of 26 months, (2) for all data, with time to toxicity taken into account and (3) at a FU of 26 months, excluding low dose ribs.

Results: The median time to fracture was 22 (range 5–51) months. Maximum rib dose best predicted fractures. The TD_{50} (dose with 50% complication) of the second NTCP model was 375 Gy. The TD_{50} was significantly higher for the other models indicating an under-estimation of the dose effect at the median follow-up time and/or when excluding low dose ribs.

Conclusions: The risk of symptomatic rib fractures after SBRT was significantly correlated to dose, and was <5% at 26 months when D_{max} < 225 Gy.

For patients with inoperable peripheral early stage non-small cell lung cancer (NSCLC), stereotactic body radiation therapy (SBRT) has become the standard of care [1,2], with good local tumor control probabilities for both primary and secondary lung tumors [3]. Toxicity rates for lung, esophagus, airway, heart and spinal cord after SBRT for NSCLC were recently reported in a review [4]. Radiation induced rib fractures are a known side effect after SBRT. Rib fractures are diagnosed clinically when a fracture is found on a follow-up (FU) CT scan. This occurs in approximately 5% of patients (range 1.6–8.3%) [5–9]. A full evaluation of all available FU CTs with extra attention to fractures yields approximately 30% of fractures (range 21–41%) [10–15]. Significant dose–effect relations were reported by several groups that used manual contouring of ribs [10–12]. However, as manual contouring is cumbersome and time consuming, this was done on a limited number of patients, or only included ribs that received high doses. Analysis of a large group of patients is warranted, and automatic segmentation of the ribs allows for such an analysis. Recently, we showed that atlas based automatic segmentation of ribs is fast, accurate and significantly equivalent to manual segmentation [16]. In this paper we use automatic segmentation of ribs for a large group of patients to determine a dose–effect relation using the Lyman–Kutcher–Burman (LKB) model. As time to toxicity is relatively long for rib fractures, i.e., 15–22 months [10–12,14], a more accurate model could be obtained when time to toxicity is taken into account.

The aim of this paper is to determine a dose–effect relation for symptomatic, radiologically diagnosed radiation induced rib fractures after SBRT for a tumor in the lung, taking into account time to toxicity.

Material/Methods

Patient and treatment characteristics

From June 2006 to June 2013 494 consecutive patients with inoperable, mostly peripheral, lung tumors were treated with SBRT to a median of 54 Gy in 3 fractions. Four-hundred and thirty-two patients had stage T1a-T2b N0 NSCLC, two patients had T2b and T3a disease, and 60 patients were treated for oligometastatic disease from primary lung, colon, prostate, breast, rectum, bladder or melanoma tumors.

Four-hundred and sixty-six patients were included (table 1); 28 patients were excluded, due to non-radiation induced fractures (2), or technical issues (26). The median tumor diameter was 2.24 cm

* Corresponding author at: Department of Radiation Oncology, Netherlands Cancer Institute, Plesmanlaan 121, 1066 CX Amsterdam, The Netherlands.
E-mail address: j.sonke@nki.nl (J.-J. Sonke).

http://dx.doi.org/10.1016/j.radonc.2017.01.004

(0.7–6.9 cm), 4% of patients had a tumor >5 cm. Eight percent of patients previously received a lobectomy, pneumonectomy or wedge resection (35). Staging of tumors was done following the 6th TNM staging system.

All patients received a mid-ventilation (before Aug 2011) or mid-position (after Aug 2011) treatment planning CT scan, derived from a 4D scan [17]. The Gross Tumor Volume (GTV) was contoured on the mid-ventilation or the mid-position scan and typically expanded anisotropically by 8 or 10 mm (depending on the breathing peak-to-peak amplitude) to generate the Planning Target Volume (PTV). For treatment planning, the Pinnacle treatment planning system (Philips Radiation Oncology Systems, Milpitas, USA) was used, where dose calculations were performed using the collapsed-cone convolution/superposition algorithm. Treatment plans consisted of 16 to 20 coplanar and noncoplanar beams for intensity modulated radiotherapy (IMRT) plans, or dual arc volumetric arc therapy (VMAT). Dose prescription allowed for inhomogeneous dose to the PTV, with a maximum dose of 165% of the prescribed dose. There were no constraints on the ribs. Three-hundred and thirty-nine patients received 54 Gy in 3 fractions (73%). Twenty-six patients received 45 Gy in 3 fractions (6%), 28 patients received multiple treatments separated by several months or years; 18 patients received two series of 54 Gy in 3 fractions (4%), 8 patients received 54 Gy in 3 fractions followed by 66 Gy in 24 fractions (2%), and two patients received two consecutive treatments of 54 Gy in 3 fractions and a series of 66 Gy in 24 fractions (0.4%). Twenty-seven percent of patients received an adapted schedule because of normal tissue constraints, overlap with a previous radiation treatment, or prior multiple RT schedules, e.g. for metachronous primary lung tumors. Other dose schedules ranged from 24 to 60 Gy in 2 to 8 fractions (14%). In one patient treated to two tumors in both lungs the third fraction was cancelled due to a pneumonia during treatment.

All patients were treated with IMRT (before Oct 2009) or VMAT (after Oct 2009) using online cone-beam guided position verification.

FU consultation consisted of a medical history, a physical examination and a CT scan at 4 months after treatment, every 6 months for two years, and yearly up to 5 years. Pain was graded using the Common Toxicity Criteria for Adverse Events (CTCAE) v3.0 [18].

Rib fractures were diagnosed on FU CT scans by the treating radiation oncologist and/or radiologist. Systematic (retrospective) evaluation of all available FU CTs was not performed, but patients that were suspected of fracture based on the CT in combination with reported pain were evaluated in detail by screening all FU CTs of these patients for fractures. Rib fractures were diagnosed radiologically and were either asymptomatic (Grade 1), or symptomatic: reported thoracic pain with intervention needed according to CTCAE criteria Grade 2 or 3. If the incidence of rib fractures was higher in patients that received multiple treatments was assessed via a student t-test.

Rib segmentation

We used atlas based segmentation in ADMIRE (2013, Elekta AB, Stockholm, Sweden) with a Random Forest implementation for rib segmentation. The method has been described previously [16,19,20]. In short, for 15 patients, the planning CTs with delineated ribcages were used as atlases. A non-rigid registration of each atlas to the planning CT of a new patient was performed, followed by a Random Forest supervised learning classification of voxels. The classification was combined with a multi-level label fusion, which merged the multiple atlas segmentations into a single new ribcage. All ribcage segmentations were manually checked for protrusions that caused connections between ribs and if necessary edited. Individual ribs were obtained from the ribcage segmentation after a triangulation of the surface mesh and separation of all unconnected surfaces, yielding 24 ribs per patient [16].

For some patients, parts of ribs 8–12 were not in the field of view of the CT. As the dose to these parts of the ribs was negligible, its influence on the NTCP model (in a smaller cohort) was negligible [16], and for these ribs only the dose on the part of the rib within the field of view was used in the calculations.

Dose–effect modeling

Physical dose distributions from the clinical plans were corrected to biologically equivalent doses, to account for the dose per fraction as given in fractions of 2 Gy (EQD2) using the linear-quadratic (LQ) model with an $\alpha/\beta = 3$ Gy [10,11,14]. For patients with synchronous tumors that were planned on a single CT scan and treated concurrently or sequentially (31 patients): either their 3D physical dose distributions were added and EQD2 corrected (concurrent), or their 3D EQD2 corrected dose distributions were

Table 1
Patient, tumor and treatment characteristics.

	Men	Women	All
No. Patients	246	220	466
Median age (range)	74 (47–91)	72 (37–89)	74 (37–91)
Median GTV volume (cc) (range)	6.3 (0.4–129)	4.55 (0.2–127)	5.46 (0.2–129)
Median PTV volume (cc) (range)	38.5 (7.1–347)	30.25 (2.3–274)	33.38 (2.3–347)
Median prescribed dose_Gy (range)	54 (24–60)	54 (24–60)	54 (24–60)
Median prescribed fractions	3 (2–8)	3 (3–8)	3 (2–8)
T stage: 1	155	147	302
T stage: 2	51	29	80
T stage: 3	1	0	1
T stage: unknown	39	44	83
Tumor location: LUL	74	80	154
Tumor location: LLL	27	34	61
Tumor location: RUL	92	63	155
Tumor location: RML	9	6	15
Tumor location: RLL	44	37	81
Median BMI (range)	25.4 (15.5–62.1)	23.4 (12.3–51.2)	24.4 (12.3–62.1)
Median FU (mo) (range)	23.3 (0.7–88.9)	28.3 (0.3–100.6)	26.1 (0.3–100.6)
No. patients with fracture ($\geqslant$G1)	32	32	64
No. patients with symptomatic fracture ($\geqslant$ G2)	26	16	42
Median time to fracture (mo) (range)	22.1 (4.5–51.2)	22.1 (9.1–41.1)	22.1 (4.5–51.2)

GTV = Gross tumor volume; PTV = Planning target volume; LUL = Left upper lobe; LLL = Left lower lobe; RUL = Right upper lobe; RML = Right middle lobe; RLL = Right lower lobe; BMI = Body mass index.

added (sequential). For patients with multiple targets (e.g. due to a metachronous primary), their planning CT scans were deformably registered (using b-splines implemented in in-house software, Worldmatch version 8.00) and their 3D EQD2 corrected doses added (30 patients). To simplify notations, EQD2 will be denoted as D in the remainder of the manuscript.

To find the optimal dose parameter to predict rib fractures, we studied three different dose parameters: the dose received by an absolute volume x of a rib, D_{x_abs}, the dose received by a relative volume x of a rib, D_{x_rel}, and the Equivalent Uniform Dose, EUD, following Eq. (1).

$$EUD = \left(\frac{1}{N}\sum_{i=1}^{N}(D_i)^{1/n}\right)^n \tag{1}$$

where N is the number of sampled volume elements in a rib, D_i is the dose in that volume element and n is the volume parameter determining the relative importance of low or high dose to the EUD [21,22].

For each rib a separate dose volume histogram (DVH) was calculated, from which dose parameters D_{x_abs} and D_{x_rel} were obtained, with x ranging from 0 to 30 cc and 0 to 100% respectively to cover small to large rib volumes. The EUD was calculated with 1/n varying from 0.1 to 500 and ∞, which emphasizes low to high doses in the rib.

The following analyses were performed twice; both for $\geqslant$G1 and $\geqslant$G2 fractures. The optimal dose parameter to predict fracture was found using Cox proportional hazard regression analysis (SPSS statistics version 22.0). Also, we included patient as random intercept to assess the inter-patient variation (the effect that ribs were grouped in 24 per patient and might not be independent). The dose parameter with the lowest log likelihood was used in a multivariate analysis using forward selection that also included other known risk factors for fracture and pain: gender and BMI [15,23,24]. Also age, lobe, T stage, COPD grade, Mean Lung Dose and GTV volume were included in the analysis. Age was not normally distributed and was therefore analyzed as a dichotomous variable, with patients divided into two groups below or above the median age.

The optimal dose parameter was used in the first NTCP model, following Eqs. (2) and (3) [21,22]:

$$NTCP = \frac{1}{\sqrt{2\pi}}\int_{-\infty}^{t} e^{-\frac{x^2}{2}dx} \tag{2}$$

$$t = \frac{D_{opt} - TD_{50}}{m \cdot TD_{50}} \tag{3}$$

where D_{opt} is the optimal dose parameter to predict a fracture, TD_{50} is the D_{opt} with 50% probability of complication and m the steepness parameter. The parameters were optimized using maximum-likelihood estimation, and their 95% CI was subsequently derived using a profile-likelihood method [25]. The probability of fracture was calculated at the median FU. Rib fractures that were diagnosed after this time point were coded as not fractured. To show the difference between NTCP curves for different FU times, the probability of fracture was also calculated at a FU time of 1, 2, 3 or 4 years.

A second NTCP model was fitted where the time to toxicity was taken into account following Tucker et al. [26]. The NTCP (Eq. (2)) was multiplied by a latency distribution for the time to toxicity, for which a log-normal distribution is assumed:

$$f(\tau) = \frac{1}{\sigma\tau\sqrt{2\pi}}e^{-(\ln\tau-\mu)^2/2\sigma^2} \tag{4}$$

where τ is the time, and μ and σ are the latency parameters. The probability of a patient experiencing toxicity at time τ was:

$$NTCP \cdot f(\tau) \tag{5}$$

The latency distribution from equation 4 was fitted to the data first, and the corresponding latency parameters μ and σ were subsequently used to optimize the parameters TD_{50} and m of Eqs. (3) and (5).

Whether all ribs, or only ribs that received high doses should be included in the NTCP model is a topic of debate [10,16], and is investigated in the Supplementary Material.

Results

In 466 patients with a median FU of 26.1 months, 64 patients (13.7%) had a total of 123 rib fractures observed on the FU CT scans, ranging from 1 to 5 fractures per patient, with maximum 1 fracture per rib. The median time to fracture was 22 months (range 5–51 months). As a typical example of a rib fracture, Fig. 1 shows a dose distribution on the planning CT and a rib fracture on the FU CT, 2.5 years after treatment.

The rib fractures were symptomatic (pain $\geqslant$G2) for 42 patients (9%) and asymptomatic (G1) for 22 patients (4.7%). Of the patients diagnosed with fractures, 35% had 1 fracture. The majority of fractures (89%) occurred in ribs 1–7. Within the 28 patients that were irradiated two or three times, 3 patients (11%) had symptomatic fractures, and 1 patient had an asymptomatic fracture (4%). This was not significantly different from the patients that were irradiated once (p-values 0.111 and 0.248 respectively). Within the 31 patients with synchronous tumors, 3 had a symptomatic fracture, which was also not significantly different from the patients that were irradiated for one tumor. From the 35 patients that had a previous thoracic surgery, 3 (9%) developed (symptomatic) fractures. All fractures were located outside of the surgical area.

In 466 patients, 11184 ribs were automatically segmented. Minimal manual editing of automatically segmented ribs required on average 2 min (1–15) per patient.

Dose parameters, D_{x_abs}, D_{x_rel} and EUD were all significantly associated with rib fracture (both $\geqslant$G1 and $\geqslant$G2) for all values of x and $1/n$ (p-values <0.001). All results shown in the remainder of the manuscript are for $\geqslant$G2 (symptomatic) fractures. Results for fractures $\geqslant$G1 are given in the Supplementary Material.

For each dose parameter the Hazard Ratios (HR) and Confidence intervals (CI) for the parameters with the lowest log likelihood values were: $D_{0\%}$, 1.014 Gy^{-1} (1.013–1.016), D_{0cc}, 1.014 Gy^{-1} (1.013–1.016) and $EUD_{1/n=\infty}$, 1.014 Gy^{-1} (1.013–1.016). The confidence intervals of the x and 1/n parameters were: x_rel 0–0.8%, x_abs 0–0.03 cc and $1/n$ 21-∞. A plot of the increasing deviances with increasing x is shown in the Supplementary Material (Fig. S1). $D_{0\%}$, D_{0cc} and $EUD_{1/n=\infty}$, are equal and will be denoted as D_{max} in the remainder of the manuscript. The random intercept was not significant, suggesting that there was no relevant interpatient variation.

The multivariate analysis showed that D_{max}, age and BMI were significantly associated with rib fractures: HR(CI): 1.014 Gy^{-1} (1.013–1.016), 1.387 (>74 year) (1.135–1.695) and 1.038 m^2/kg (1.001–1.077) respectively.

The D_{max} was used for NTCP modeling. At the median FU of 26 months, 230 patients were alive or had suffered a fractured rib, resulting in 5520 included ribs with 54 fractures for the first NTCP model. The incidence of rib fractures as a function of D_{max} and the most likely fit of the LKB model at 26 months are shown in Fig. 2, and corresponding optimal LKB parameters in Table 2 (column 1). The risk to develop a rib fracture at 26 months or before that was <5% when the D_{max} < 207 Gy (Fig. 2A), and <50% when D_{max} < 452 Gy. The average D_{max} of the fractured ribs that were found before the median FU was not significantly different from the average D_{max} of the fractured ribs that were found after the median FU.

The difference between NTCP curves for different FU times is shown in Fig. 2B. The steepness of the dose–effect relation

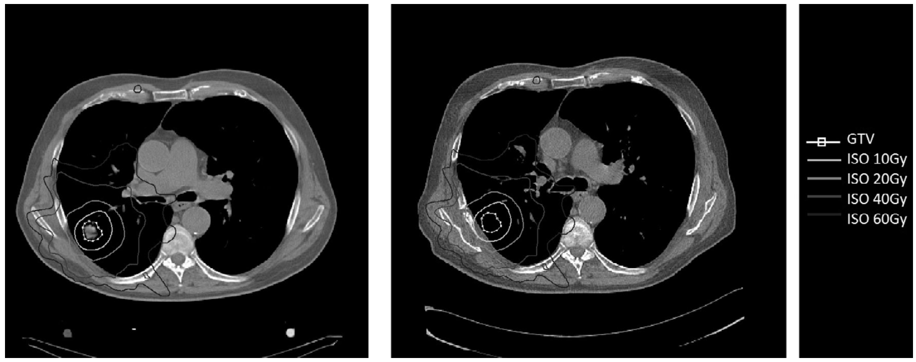

Fig. 1. IMRT dose plan for a 72 year old male with a 9.4 cc (2.6 cm diameter) NSCLC in the left upper lobe (left), and a rib fracture visible on FU CT at 33 months (right). GTV (dashed line), iso-dose lines (solid).

Table 2
Optimal dose parameters for 3 NTCP models: (1) all data at 26 months. (2) all data included, and time to toxicity taken into account.

	NTCP model 1 (5928 ribs) FU 26 months	NTCP model 2 (11184 ribs) time to toxicity incorporated
TD_{50} (Gy)	452 (420–482)	375 (351–398)
m	0.329 (0.313–0.346)	0.348 (0.332–0.365)
μ		3.44 (3.20–3.68)
σ		0.695 (0.567–0.823)

increases with increasing FU times. This is associated with an increasing m parameter, and a decreasing TD_{50} parameter (Supplementary Material Table S1).

The second NTCP model (Table 2, column 2), where the time to toxicity is taken into account, gives a prediction of developing fractures over time (Supplementary Material, Fig. S2). Fig. 3 shows the incidence of rib fractures over time and the predicted incidence for 4 different dose levels. In the highest dose bin (average D_{max} = 334 Gy), the risk of fracture at the median FU of 26 months was 14%. The risk of rib fractures at 26 months was < 5% when the D_{max} < 225 Gy, and < 50% when D_{max} < 375 Gy.

Fig. 4 shows that with longer FU, the 5% chance of fracture is reached at a decreasingly lower dose. For clinical interpretation we show the chance of fracture for different physical doses and fractionation schemes in the Supplementary Materials (Fig. S3).

Discussion

We used automatic segmentation of ribs to analyze all ribs in a large cohort of patients with a lung tumor, treated with SBRT, and determined a dose–effect relation for radiation induced rib fractures. Four-hundred and sixty-six patients were included in the dosimetric analysis, making this, to our knowledge, the largest dose–effect analysis of rib fractures to date.

Both NTCP models described in our paper, excluding or including time to toxicity, show a clear dose–effect relationship to develop a rib fracture, and predict a 5% chance of fractures at 26 months for ribs receiving at least 207 or 225 Gy respectively. However, the differences between the models should not be ignored. The study population consisting of patients with medically inoperable primary or oligo metastatic pulmonary lesions have a relatively short median overall survival in relation to the median time to toxicity. Therefore, in a standard NTCP model the interpretation of the calculated probabilities is difficult, as the model is only valid for the one time point that was chosen. Also, in a standard NTCP model the chance to develop a fractured rib increases to 100% for high doses, which possibly is not valid for that time point. The second model not only predicts the chance of fracture, but the chance of fracture over time (Fig. 3). It shows that the chance of fracture increases both over time and with higher doses. This model only approaches a 100% chance of rib fractures for high doses and long follow-up times. When modeling the chance of fractures in time, the model that includes time to

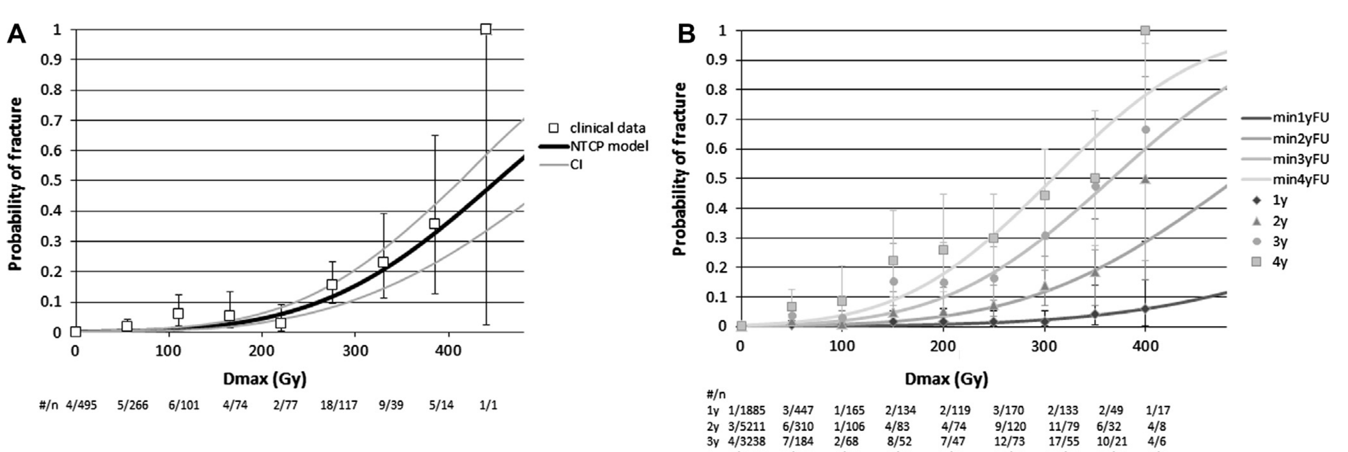

Fig. 2. (A) The incidence of rib fractures for ribs at 26 months FU (the median FU), or an earlier fracture, as a function of the D_{max} and the optimized NTCP model indicating a clear dose–effect relationship. Displayed below are the number of included ribs (n) and number of fractured ribs (#). (B). The incidence of rib fractures at different minimal FU times as a function of the D_{max} and the optimized NTCP model. Displayed below are the number fractured ribs (#), and the number of included ribs (n) for the different minimal FU times.

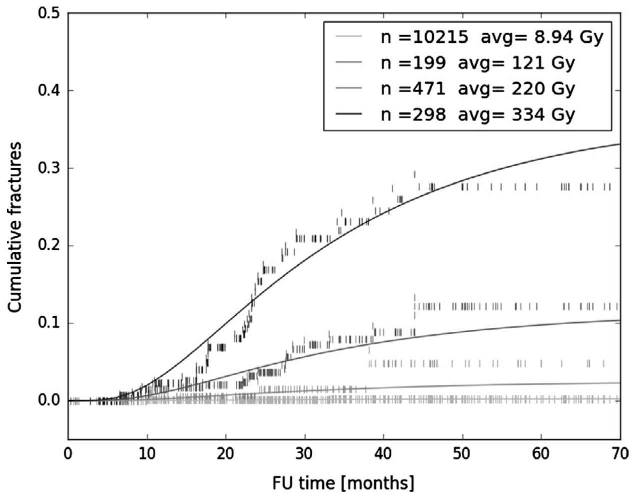

Fig. 3. Kaplan –Meier curve for rib fractures for D_{max} in 4 different groups: actual (crosses), and predicted (lines).

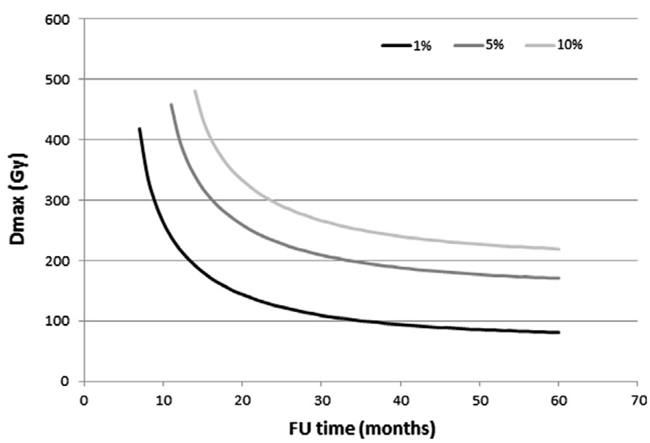

Fig. 4. Isoprobability lines for the 1%, 5% and 10% chance of ⩾G2 fracture as a function of FU time.

toxicity only requires 4 parameters: TD_{50}, m, μ and σ, while the standard model requires a TD_{50} and m at each time point, so 8 parameters to create the 4 time points in Fig. 2B. Comparing the two models quantitatively is not straight forward, as they use different data as input in the model; the second model, that includes time to toxicity, incorporates all fractures that were found (at any time point). The first model ignores all fractures that were found after the chosen time point. The second model facilitates the determination of the chance of fracture at *any* time point. Therefore we believe that both clinically and mathematically, the second model that includes time to toxicity is the most useful model.

The best predictor for a fracture is a high dose to a small rib volume: $D_{0.5cc}$ [11], D_{2cc} [10] or D_{max} (this paper). The confidence interval of x in D_{x_abs} was 0–0.03 cc, which makes our result significantly different from the results reported by Pettersson et al. and Taremi et al. [10,11]. Other dosimetric parameters, such as D_{mean} were also significantly associated with rib fracture. For vertebral fractures a similar association exists between fractures and the D_{mean} [27,28], where fractures were predominantly seen in the high-dose region [29]. Associations between D_{max} and vertebral fracture were not reported. The average D_{max} for fractures found before or after the median FU was not significantly different, which indicated that the lower doses did not have a later effect than the higher doses.

In this paper, we use planned D_{max} to build an NTCP model. Geometrical uncertainties in the treatment of lung cancer patients, such as setup errors, baseline shifts and respiratory motion affect the delivered dose to the rib. As D_{max} is more sensitive to geometrical uncertainties than other dose parameters, it is somewhat surprising that the planned D_{max} is still the optimal parameter. Extensive dose accumulation studies are required to gain further insight in the impact of geometrical uncertainties on NTCP modeling accuracy.

A shortcoming of this study is that we did not perform a full retrospective evaluation of all FU CTs, as this was not feasible for this large group of patients. Also, FU CTs were not available for a subset of patients. However, at our institute patients with reported pain were screened for fractures on their CT during normal clinical routine. Therefore we feel confident that the reported number of ⩾G2 fractures approximates the true incidence. The ⩾G1 rib fractures in our cohort are presumably underreported, but as a G1 fracture is clinically less relevant, we focused our work on the ⩾G2 fractures. However, to compare our optimal LKB parameters to literature, we also looked at the ⩾G1 rib fractures, as these values were not reported for the ⩾G2 rib fractures.

Comparing the optimal LKB parameters to predict ⩾G1 rib fractures with previously reported values gives higher values for the TD_{50} than Taremi et al. [11] and Stam et al. [16]. In the first paper, the 50% risk of rib fractures at the median FU of 25 months, estimated from their Fig. 4, is at $D_{0.5Gy}$ 60 Gy physical dose in 3 fractions, which equals 276 Gy EQD2-corrected dose [11]. Our TD_{50} at the median FU of 26 months for the ⩾G1 fractures was 406 Gy (following the first model, which does not take time to toxicity into account, as Taremi et al. [11] also did not). However, in their paper a systematic review of all available CTs was performed to obtain all (a)symptomatic fractures, while in our paper only fractures diagnosed during normal clinical routine were included. Therefore it is to be expected that our lower fracture rate and the lower risk of fractures is represented by a higher TD_{50} in our paper.

Our 9% ⩾G2 fracture rate falls within the wide ranges reported in the literature for ⩾G2 fractures; reported fracture rates are 24%, 10%, 2% and 0% [11,12,14,30]. Our LKB parameter values are within the rather wide confidence intervals reported previously, as those paper only included 41 and 57 patients [10,16].

In our multivariate analysis, we included only one dosimetric parameter to avoid multicollinearity. The dose to the rib was significantly associated with fracture, as were age and BMI. COPD grade, which is correlated to the use of corticoid steroids, was not associated with fracture. Distance from rib to tumor was not incorporated in the multivariate analysis, as it is strongly correlated to rib dose. Gender, which proved significantly associated with rib fracture after SBRT in other studies [11,15,23], was not significant in our group of patients. The higher risk in female patients was previously attributed to the higher risk of osteoporosis in these patients [23]. Due to the retrospective nature of this study, clinical factors such as osteoporosis status or diabetes mellitus were only known for a small subset of patients, and could thus not be assessed in this study, but we encourage future research to include these in a multivariate analysis.

Previously we discussed whether an NTCP model based on absolute or relative volumes would be more accurate [16], and how a larger dataset could answer this question. Within our large dataset, D_{max} was the best predictor for fractures, making the discussion on absolute or relative volumes superfluous.

We did not include a V_x parameter (volume receiving dose x) in our NTCP modeling, as there are many ribs that receive a low dose. The V_x of these ribs would be zero for a large range of x which is unfavorable for NTCP modeling, and D_x typically outperforms V_x in such situations [31].

In only 9% of patients in this cohort, did rib fractures cause pain complaints (⩾G2). One third of the fractures were asymptomatic (G1). Different fractionation schemes could be applied to possibly reduce the chance of rib fractures [32]. However, since in this cohort the vast majority of the patients received 54 Gy in 3 fractions, the effect of a different scheme on the incidence of rib fracture could not be tested. However, this study has caused us to reconsider our fractionation scheme for tumors close to the rib, as did Bongers et al. [8]. When applying a different fractionation scheme, the chance of fracture can easily be calculated using our model, as it only needs the EQD2-corrected D_{max}. In this cohort, patients that were irradiated twice for synchronous or metachronous tumors did not have a significantly higher chance to develop a rib fracture, indicating that the EQD2-corrected D_{max} is the dominant prognostic factor in predicting fracture. In clinical practice, informing the patient not only about the chance of developing a rib fracture, but also about the duration of the pain is relevant. In this dataset, it was not feasible to study the duration of pain, as the frequency of the FU CT scans was too low.

Conclusion

We used automatic segmentation of ribs in a large group of patients with a lung tumor, treated with SBRT, and determined a dose–effect relation for radiation induced rib fractures. The risk of symptomatic rib fracture was significantly correlated to the administered dose, and was <5% at 26 months when the EQD2-corrected D_{max} was lower than 225 Gy.

Conflict of interest

This work was sponsored in part by a research grant from Elekta Oncology Systems Ltd.

Acknowledgement

This work was sponsored in part by a research grant from the Dutch Cancer Society (NKI 2009-4568).

Appendix A. Supplementary data

Supplementary data associated with this article can be found, in the online version, at http://dx.doi.org/10.1016/j.radonc.2017.01.004.

References

[1] Baumann P, Nyman J, Hoyer M, Wennberg BM, Gagliardi G, Lax I, et al. Outcome in a prospective phase II trial of medically inoperable stage I non-small-cell lung cancer patients treated with stereotactic body radiotherapy. J Clin Oncol 2009;27:3290–6.
[2] Nyman J, Hallqvist A, Lund J-Å, Brustugun O-T, Bergman B, Bergström P, et al. SPACE – a randomized study of SBRT vs conventional fractionated radiotherapy in medically inoperable stage I NSCLC. Radiother Oncol 2016;121:1–8.
[3] Guckenberger M, Klement RJ, Allgäuer M, Andratschke N, Blanck O, Boda-Heggemann J, et al. Local tumor control probability modeling of primary and secondary lung tumors in stereotactic body radiotherapy. Radiother Oncol 2016;118:485–91.
[4] Fleming C, Cagney DN, O'Keeffe S, Brennan SM, Armstrong JG, McClean B. Normal tissue considerations and dose-volume constraints in the moderately hypofractionated treatment of non-small cell lung cancer. Radiother Oncol 2015;119:423–31.
[5] Onishi H, Shirato H, Fujino M, Hayakawa K, Takeda A, Ouchi A, et al. Hypofractionated stereotactic radiotherapy (HypoFXSRT) for Stage I non-small cell lung cancer: Updated results of 257 patients in a Japanese multi-institutional study. J Thorac Oncol 2007;2:94–100.
[6] Grills IS, Hope AJ, Guckenberger M, Kestin LL, Werner-Wasik M, Yan D, et al. A collaborative analysis of stereotactic lung radiotherapy outcomes for early-stage non-small-cell lung cancer using daily online cone-beam computed tomography. J Thorac Oncol 2012;7:1382–93.
[7] Andolino DL, Forquer JA, Henderson MA, Barriger RB, Shapiro RH, Brabham JG, et al. Chest wall toxicity after stereotactic body radiotherapy for malignant lesions of the lung and liver. Int J Radiat Oncol Biol Phys 2011;80:692–7.
[8] Bongers EM, Haasbeek CJA, Lagerwaard FJ, Slotman BJ, Senan S. Incidence and risk factors for chest wall toxicity after risk-adapted stereotactic radiotherapy for early-stage lung cancer. J Thorac Oncol 2011;6:2052–7.
[9] Mutter RW, Liu F, Abreu A, Yorke E, Jackson A, Rosenzweig KE. Dose–volume parameters predict for the development of chest wall pain after stereotactic body radiation for lung cancer. Int J Radiat Oncol Biol Phys 2011:1–8.
[10] Pettersson N, Nyman J, Johansson K. Radiation-induced rib fractures after hypofractionated stereotactic body radiation therapy of non-small cell lung cancer: a dose- and volume-response analysis. Radiother Oncol 2009;91:360–8.
[11] Taremi M, Hope AJ, Lindsay P, Dahele MR, Fung S, Purdie TG, et al. Predictors of Radiotherapy Induced Bone Injury (RIBI) after stereotactic lung radiotherapy. Radiat Oncol 2012;7:159.
[12] Asai K, Shioyama Y, Nakamura K, Sasaki T, Ohga S, Nonoshita T, et al. Radiation-induced rib fractures after hypofractionated stereotactic body radiation therapy: risk factors and dose–volume relationship. Int J Radiat Oncol Biol Phys 2012;84:768–73.
[13] Nambu A, Onishi H, Aoki S, Koshiishi T, Kuriyama K, Komiyama T, et al. Rib fracture after stereotactic radiotherapy on follow-up thin-section computed tomography in 177 primary lung cancer patients. Radiat Oncol 2011;6:137.
[14] Miura H, Inoue T, Shiomi H, Oh R-J. Differences in rates of radiation-induced true and false rib fractures after stereotactic body radiation therapy for Stage I primary lung cancer. J Radiat Res 2014:1–6.
[15] Kim SS, Song SY, Kwak J, Ahn SD, Kim JH, Lee JS, et al. Clinical prognostic factors and grading system for rib fracture following stereotactic body radiation therapy (SBRT) in patients with peripheral lung tumors. Lung Cancer 2013;79:161–6.
[16] Stam B, Peulen H, Rossi MMG, Belderbos JSA, Sonke J-J. Validation of automatic segmentation of ribs for NTCP modeling. Radiother Oncol 2016;118:528–34.
[17] Wolthaus JWH, Sonke J-J, van Herk M, Belderbos JSA, Rossi MMG, Lebesque JV, et al. Comparison of different strategies to use four-dimensional computed tomography in treatment planning for lung cancer patients. Int J Radiat Oncol Biol Phys 2008;70:1229–38.
[18] Trotti A, Colevas AD, Setser A, Rusch V, Jaques D, Budach V, et al. CTCAE v3.0: development of a comprehensive grading system for the adverse effects of cancer treatment. Semin Radiat Oncol 2003;13:176–81.
[19] Han X. Learning-boosted label fusion for multi-atlas auto-segmentation. Mach Learn Med Imaging 2013;8184:17–24.
[20] Han X, Hoogeman MS, Levendag PC, Hibbard LS, Teguh DN, Voet P, et al. Atlas-based auto-segmentation of head and neck CT images. In: Medical image computing and computer-assisted intervention – MICCAI 2008, vol. 11. New York, NY, USA: Springer Berlin Heidelberg; 2008(Pt 2):434–41.
[21] Lyman JT. Complication probability as assessed from dose-volume histograms. Radiat Res 1985;104:S13.
[22] Kutcher GJ, Burman C. Calculation of complication probability factors for non-uniform normal tissue irradiation: the effective volume method Gerald. Int J Radiat Oncol Biol Phys 1989;16:1623–30.
[23] Nambu A, Onishi H, Aoki S, Tominaga L, Kuriyama K, Araya M, et al. Rib fracture after stereotactic radiotherapy for primary lung cancer: prevalence, degree of clinical symptoms, and risk factors. BMC Cancer 2013;13:68.
[24] Welsh JS, Thomas J, Shah D, Allen PK, Wei X, Mitchell K, et al. Obesity increases the risk of chest wall pain from thoracic stereotactic body radiation therapy. Int J Radiat Oncol Biol Phys 2011;81:91–6.
[25] Venzon DJ, Moolgavkar SH. A method for computing profile-likelihood-based confidence intervals. Appl Stat 1988;37:87–94.
[26] Tucker SL, Liu HH, Liao Z, Wei X, Wang S, Jin H, et al. Analysis of radiation pneumonitis risk using a generalized Lyman model. Int J Radiat Oncol Biol Phys 2008;72:568–74.
[27] Uyterlinde W, Chen C, Belderbos J, Sonke J-J, Lange C, de Bois J, et al. Fractures of thoracic vertebrae in patients with locally advanced non-small cell lung carcinoma treated with intensity modulated radiotherapy. Radiother Oncol 2016;118:437–41.
[28] Otani K, Teshima T, Ito Y, Kawaguchi Y, Konishi K, Takahashi H, et al. Risk factors for vertebral compression fractures in preoperative chemoradiotherapy with gemcitabine for pancreatic cancer. Radiother Oncol 2016;118:424–9.
[29] Pilz K, Hoffmann AL, Baumann M, Troost EGC. Vertebral fractures – an underestimated side-effect in patients treated with radio(chemo)therapy. Radiother Oncol 2016;118:421–3.
[30] Aoki M, Sato M, Hirose K, Akimoto H, Kawaguchi H, Hatayama Y, et al. Radiation-induced rib fracture after stereotactic body radiotherapy with a total dose of 54–56 Gy given in 9–7 fractions for patients with peripheral lung tumor: impact of maximum dose and fraction size. Radiat Oncol 2015;10:99.
[31] Hope AJ, Lindsay PE, El Naqa I, Alaly JR, Vicic M, Bradley JD, et al. Modeling radiation pneumonitis risk with clinical, dosimetric, and spatial parameters. Int J Radiat Oncol Biol Phys 2006;65:112–24.
[32] Lagerwaard FJ, Verstegen NE, Haasbeek CJA, Slotman BJ, Paul MA, Smit EF, et al. Outcomes of Stereotactic ablative radiotherapy in patients with potentially operable stage I non-small-cell lung cancer. Int J Radiat Oncol Biol Phys 2011;83:348–53.